

## Practical challenges in adaptive Marchenko imaging

Joost van der Neut, Kees Wapenaar, Jan Thorbecke and Evert Slob (Delft University of Technology)

### SUMMARY

Through the multidimensional Marchenko equation, seismic redatuming can be expressed as a series. Unlike in conventional redatuming, where only the first term of these series is evaluated, not only primary reflections, but all orders of internal multiples are taken into account by this approach. By crosscorrelation of the redatumed wavefields with their corresponding (direct) source wavefields, as computed in a macro velocity model, a seismic image can be obtained without artifacts from internal multiples. Unfortunately, this approach requires accurate knowledge of the source signature, which is not always available. Moreover, the method is sensitive for source / receiver ghosts, coupling effects, attenuation and other noise. In practice, the individual terms in the series can also be added adaptively. This procedure is successful if internal multiples don't interfere with primary reflections, but has its limitations in more complex media. In this contribution, we analyze the feasibility of adaptive addition, using only the first two terms in the series. The result appears useful for internal multiple suppression, as we illustrate on synthetic data with severe event interference and on field data.

### INTRODUCTION

In Reverse Time Migration (RTM), seismic data are propagated backwards in time from the Earth's surface to image points in the subsurface, using finite-difference computations in a smooth macro velocity model. An image is created by crosscorrelation of these backpropagated receiver wavefields with their associated source wavefields, which are propagated forwards in time from the source locations. An equivalent result can be obtained by redatuming the recorded data to every image point in the subsurface using pre-computed Green's functions and crosscorrelating these redatumed data with their associated source wavefields (Esmersoy and Oristaglio, 1988; Schuster, 2002). Although RTM has been very successful in imaging primary reflections, it is not able to handle internal multiples, given that the macro model is generally smooth and does not contain information on the subsurface reflectivity. As a consequence, internal multiples are imaged at erroneous locations, causing artifacts in the RTM image.

Recently, it was shown how up- and downgoing wavefields inside the subsurface can be computed through the multidimensional Marchenko equation, using seismic reflection data and a macro velocity model (Wapenaar et al., 2014). By multidimensional deconvolution of the retrieved upgoing wavefields with the downgoing wavefields at each depth level, an image can be obtained, where not only primary reflections, but also all orders of internal multiples contribute to the retrieved reflectivity (Behura et al., 2014; Brogini et al., 2014). Meles et al. (2015) showed how internal multiples can also

be predicted and removed by combining the Marchenko equation with seismic interferometry. Alternatively, we use the Marchenko framework to replace the receiver wavefields in conventional RTM. By retrieving the upgoing wavefields at each image point through the Marchenko equation and crosscorrelating these with their associated (direct) source wavefields, an image can be constructed, which is similar to the RTM result, but lacks the artifacts caused by internal multiples.

### MARCHENKO REDATUMING

Wapenaar et al. (2014) showed how up- and downgoing wavefields in the subsurface can be retrieved through an iterative scheme. By adding the update of each iteration subsequently, it follows that these wavefields can be expressed as a series. For the upgoing wavefield, we can write these series as

$$\mathbf{u} = \mathbf{u}_0 + \sum_{k=1}^{\infty} \mathbf{u}_k. \quad (1)$$

In this notation,  $\mathbf{u}$  is a vector of concatenated traces that describe the upgoing wavefield at a specified image point in the subsurface for all source locations at the surface. The first term in these series,  $\mathbf{u}_0$ , is the upgoing wavefield that we would obtain by conventional seismic redatuming. It can be retrieved by evaluating (Berryhill, 1984; Van der Neut et al., 2015):

$$\mathbf{u}_0 = \Psi \mathbf{R} \mathbf{f}_d. \quad (2)$$

Here,  $\mathbf{f}_d$  is introduced as the initial focusing function. It contains time-reversed Green's functions (computed in the macro model) from all source locations to the subsurface image point. The elements of  $\mathbf{f}_d$  are arranged in a similar fashion as those of vector  $\mathbf{u}$ , but are reversed in time. Matrix  $\mathbf{R}$  applies multidimensional convolution of these time-reversed Green's functions with the recorded data at the surface. Finally, we have introduced a mask matrix  $\Psi$  to truncate the output. This matrix removes all information before the direct wavefield. The required truncation times for this operation are obtained from the initial focusing function  $\mathbf{f}_d$ .

A conventional RTM image can be obtained by crosscorrelating  $\mathbf{u}_0$  with the associated source wavefield at each image point. With this approach, primary reflections are migrated correctly, but internal multiples are not. This can be understood intuitively, since  $\mathbf{u}_0$  is not the exact upgoing wavefield in the subsurface, but an approximation, where the series in equation 1 have been truncated after the first term. To be more specific:  $\mathbf{u}_0$  contains all physical upgoing reflections that populate  $\mathbf{u}$ , but is contaminated with spurious events, stemming from internal multiples in the overburden. These spurious events are suppressed by the other terms in the series, which can be expressed as (Wapenaar et al., 2014; Van der Neut et al., 2015):

### Practical challenges in adaptive Marchenko imaging

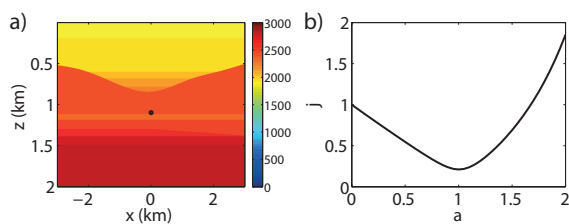


Figure 1: a) Synthetic 2D model (with propagation velocities in  $m/s$ ). The black dot indicates the reference image point. b) Function  $j$  evaluated for various scaling factors  $a$  of the reflection data that was computed in this model. The series in Equation 1 has been truncated at  $k = 10$ .

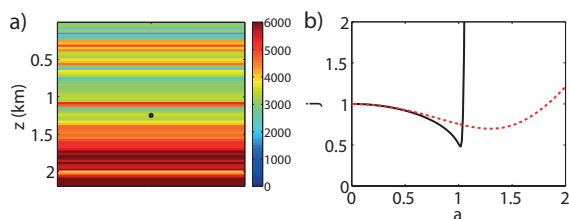


Figure 2: a) Synthetic 1D model (with propagation velocities in  $m/s$ ). The black dot indicates the reference image point. b) In solid black: function  $j$  evaluated for various scaling factors  $a$  of the reflection data that was computed in this model. The series in Equation 1 has been truncated at  $k = 50$ . In dashed red: same, where the series has been truncated at  $k = 1$ .

$$\mathbf{u}_k = \Psi \mathbf{R} (\Theta \mathbf{R}^* \Theta \mathbf{R})^k \mathbf{f}_d. \quad (3)$$

Matrix  $\mathbf{R}^*$  has a similar structure as  $\mathbf{R}$ , but it applies multidimensional crosscorrelation (rather than convolution) with the reflection data. Matrix  $\Theta$  is complimentary to  $\Psi$  in the sense that  $\Psi + \Theta = \mathbf{I}$ . This matrix removes all information after the direct wavefield (including the direct wavefield itself). Both  $\Theta$  and  $\Psi$  are symmetric in time, meaning that they apply similar truncations to the acausal part of any wavefield as they do to the causal part. If the correct upgoing wavefield  $\mathbf{u}$  (rather than approximation  $\mathbf{u}_0$ ) would be crosscorrelated with the source wavefield at each image point, an equivalent RTM image can be constructed without artifacts from internal multiples.

#### MINIMUM-ENERGY CRITERION

Evaluation of the series in Equation 1 requires accurate knowledge of the exact amplitudes of the reflection data that constitute the matrices  $\mathbf{R}$  and  $\mathbf{R}^*$ . To illustrate this, we use Equation 1 to retrieve the upgoing Green's function at a reference image point in a 2D synthetic model that is shown in Figure 1a. More information on this model and the acquisition parameters can be found in Wapenaar et al. (2014). In our example, we rescale the data with a coefficient  $a$ , prior to redatuming. For various values of  $a$ , we have evaluated the following (cost) function, using the redatumed data:

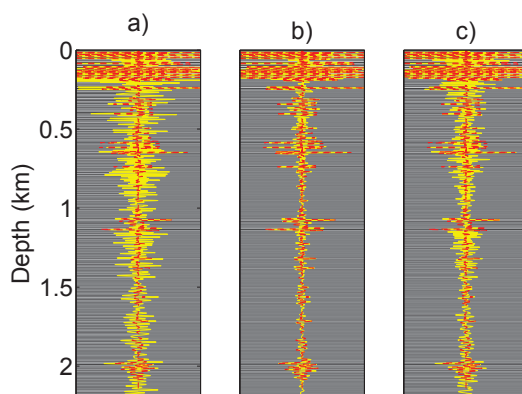


Figure 3: a) Image of  $\mathbf{u}_0$  (solid yellow + left half of gray scale) versus the image of data without internal multiples (dashed red + right half of gray scale). b) Similar image of  $\mathbf{u}$  that we retrieved with Equation 1, truncated at  $k = 50$ , using the exact reflection response. c) Image of  $\mathbf{u}_0$  after adaptive addition of  $\mathbf{u}_1$ .

$$j = \frac{|\mathbf{u}|_2}{|\mathbf{u}_0|_2}. \quad (4)$$

Here,  $|\mathbf{u}|_2$  and  $|\mathbf{u}_0|_2$  are the  $l_2$ -norms of  $\mathbf{u}$  and  $\mathbf{u}_0$ , being measures for the overall ‘energy’ in these gathers. The resulting  $j$  is shown in Figure 1b, where Equation 1 has been evaluated up to  $k = 10$ . We immediately observe a well-defined minimum at  $a = 1$ , being its true value. When  $a$  is too small, updates are under-predicted, resulting in an incomplete removal process of the spurious events that are embedded in  $\mathbf{u}_0$ . If  $a$  is too large, updates are over-predicted, such that extra information is added to the gathers (rather than subtracted). As Figure 1b suggests,  $j$  seems to be a useful cost function to determine  $a$ , even if the data are erroneously scaled. Extending this idea,  $a$  could be replaced by a short adaptive filter that minimizes cost function  $j$ . In that way, mismatches in the predicted updates can be compensated, even if they are frequency-dependent. In various other demultiple methods, adaptive filters have proven very useful, especially in field data applications (Verschuur and Berkhout, 1997; Luo et al., 2011).

The success of adaptive filters depends strongly on satisfying the minimum-energy criterion of cost function  $j$ . In severely complex media, the interference of events can obstruct the adaptive procedure. To illustrate this problem, we have repeated the previous experiment in a complex 1D model, see Figure 2a. More information on this model can be found in Alexandrov et al. (2012). Even in this complex model with severe event interferences, we find a clear minimum of the cost function at  $a = 1$ , as shown by the solid black line in Figure 2b (where we evaluated up to  $k = 50$ ). It should be noticed, though, how rapidly  $j$  increases if  $a$  is just slightly higher than 1, indicating a high sensitivity for over-scaling the data. Another important notification is that solving for  $a$  is in essence a nonlinear problem. As a crude approximation, we can truncate the series at  $k = 1$ . As a consequence, solving for  $a$  becomes a linear problem. The dashed line in Figure 2b shows

## Practical challenges in adaptive Marchenko imaging

$j$  for this particular case. Although the observed minimum is clearly not at  $a = 1$  (and does not provide a solution to the exact Marchenko equation), solving this minimization problem locally can still serve as valuable input for internal multiple suppression. To illustrate this, we have retrieved the upgoing wavefield at each depth level of the model and computed an image by crosscorrelation with the associated source pulse. In Figure 3a, we show the result (in solid yellow) for the migration of  $\mathbf{u}_0$ . This result can be interpreted as a 1D RTM image. We compare this result with an equivalent image of a reference dataset with only primaries (in dashed red). We observe a significant amount of artifacts in the image of  $\mathbf{u}_0$ , mainly stemming from the strong contrasts in the shallow part of the model, emerging as spurious events in the redatumed data. In Figure 3b, we show the image of  $\mathbf{u}$ , which is obtained with Equation 1, truncated at  $k = 50$ , using the correct scaling of the reflection response ( $a = 1$ ). Note that most of the artifacts have been removed from the image, confirming the effectiveness of Marchenko redatuming. In Figure 3c, we show an equivalent result, where only the first update  $\mathbf{u}_1$  has been added adaptively to  $\mathbf{u}_0$ . In this example, we have used a scalar adaptive filter that was applied in a local sliding window of 50ms. Although we have not been able to obtain the accuracy that we demonstrated in Figure 3b, we still have achieved a significant improvement compared to imaging  $\mathbf{u}_0$ , even with the high level of event interference that characterizes this model.

### APPLICATION TO FIELD DATA

To evaluate the performance of adaptive Marchenko imaging in practice, we test the procedure on marine streamer data. More information on these data and the acquisition parameters can be found in Altheyab et al. (2013). For our current study, we select a relatively simple part of the data, covering 2.5km at the surface. The source signature has been deconvolved from these data and free-surface multiples have been removed. Further, we have gained the data by  $\sqrt{t}$  to mimic a 2D situation (accounting for 3D geometrical spreading) and we interpolated the near offsets by NMO-correction and cubic spline interpolation, following Verschuur (1991). First, we redatumed the recorded data in a macro velocity model with Equation 2, leading to an initial estimate of the upgoing wavefield  $\mathbf{u}_0$  at each image point. A conventional RTM image is obtained by crosscorrelating these data with source wavefields that were computed in the same macro model. This image is shown in Figure 4a, with a zoomed section in Figure 5a. Two artifacts of internal multiples have been indicated by the red and yellow arrows. Their origin is explained by the dashed red and yellow raypaths in the figure. We aim to remove these artifacts by adding the second term  $\mathbf{u}_1$  in Equation 1 to our initial estimate of the upgoing wavefield  $\mathbf{u}_0$ . Since imaging is a linear process, we can migrate  $\mathbf{u}_1$  separately and add the result to the RTM image of  $\mathbf{u}_0$ , as we will do in this example. The image of  $\mathbf{u}_1$  is shown in Figure 4b, with a zoomed section in Figure 5b. The red and yellow arrows indicate the events that are supposed to cancel the artifacts in Figures 4a and 5a. Unfortunately, the amplitudes are incorrect and the events are slightly out of phase. This can be due to various reasons, such

as incorrect near-offset interpolation, frequency-dependent attenuation, unaccounted 3D effects, incorrect deconvolution of the source signature, incorrect deghosting or other noise. We try to account for these effects by an adaptive filter that enforces minimum energy when the images of  $\mathbf{u}_0$  and  $\mathbf{u}_1$  are added together. The filter is 5 samples long and applied in a local sliding window of 750m by 750m. In Figures 4c and 5c, we show the image of  $\mathbf{u}_1$ , after applying the filter. Although the signals are slightly more in phase, a complete subtraction process of the artifacts in the image of  $\mathbf{u}_0$  is still cumbersome. This is illustrated in Figures 4d and 5d, where the images of  $\mathbf{u}_0$  and  $\mathbf{u}_1$  are added (after the adaptive filter). Although the event that is marked in yellow has clearly been subtracted to some extent, this process has been incomplete. The event that is marked in red seems also to be weakened, but this observation is hindered by various interferences, making it hard to draw a definite conclusion here.

### CONCLUSION

The multidimensional Marchenko equation can be solved by evaluating a series, which can be used for redatuming a seismic wavefield from the surface to an image point in the subsurface. In conventional seismic redatuming, only the first term of the series is evaluated. Although this term inherits all physical upgoing reflections, it can also contain spurious events that are caused by internal multiples in the overburden. These spurious events can be eliminated from the redatumed data by evaluating the remainder of the series. By assuming that the redatumed data has minimum energy after subtracting the spurious events, the terms in the series can be added adaptively. We have shown that this minimum-energy criterion is often satisfied, even in severely complex models. However, finding the adaptive filters is essentially a non-linear problem. A crude approximation can be made by summing only the first two terms in the series adaptively. Even in relatively complex media with strong event interferences, this approach enabled us to suppress artifacts from internal multiples. Care should be taken, especially with aggressive long filters applied in short windows, since primary reflections can be accidentally eliminated, as we know from other methods that use minimum-energy criteria. Finally, we have demonstrated how artifacts from internal multiples can be suppressed in a RTM image of marine streamer data, using the adaptive Marchenko redatuming strategy. Although this suppression was incomplete, more accurate preprocessing is likely to improve these results.

### ACKNOWLEDGEMENTS

This research is sponsored by the Technology Foundation STW, applied science foundation of NWO (project 13078). We thank Saudi Aramco for sharing the 1D synthetic model. Finally, we thank Jerry Schuster, Abdullah Altheyab, Xin Wang, Bowen Guo and Gaurav Dutta (all KAUST) for their collaboration.

Practical challenges in adaptive Marchenko imaging

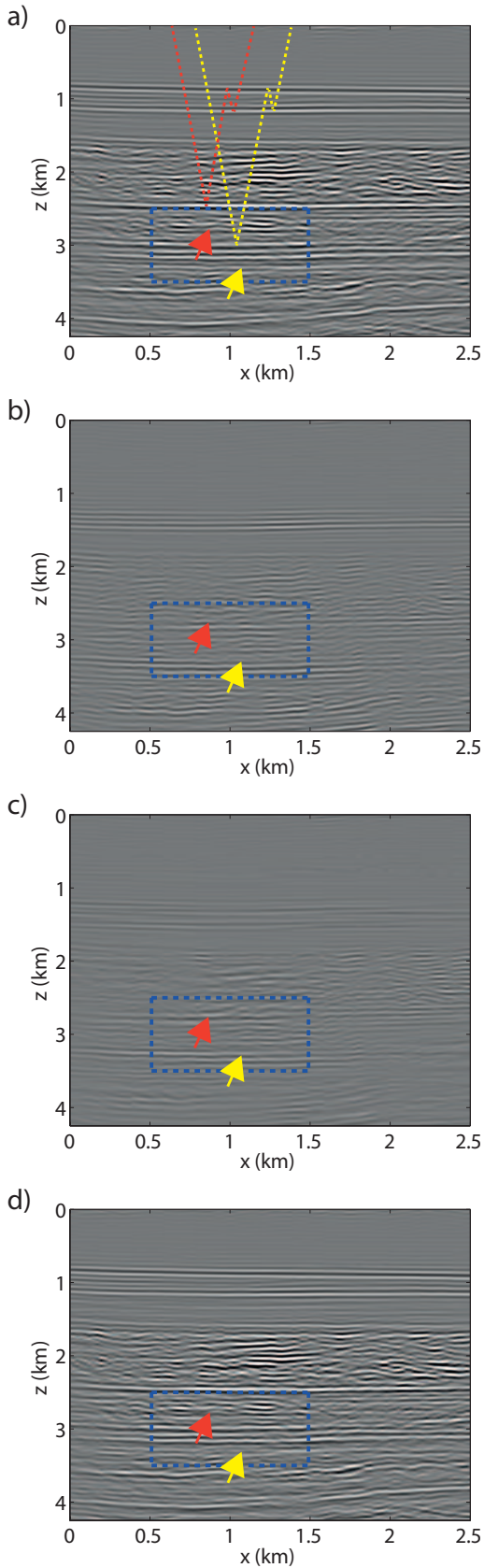


Figure 4: Images of a)  $u_0$ , b)  $u_1$ , c)  $u_1$  after adaptive filtering and d)  $u_0 + u_1$  after adaptive filtering.

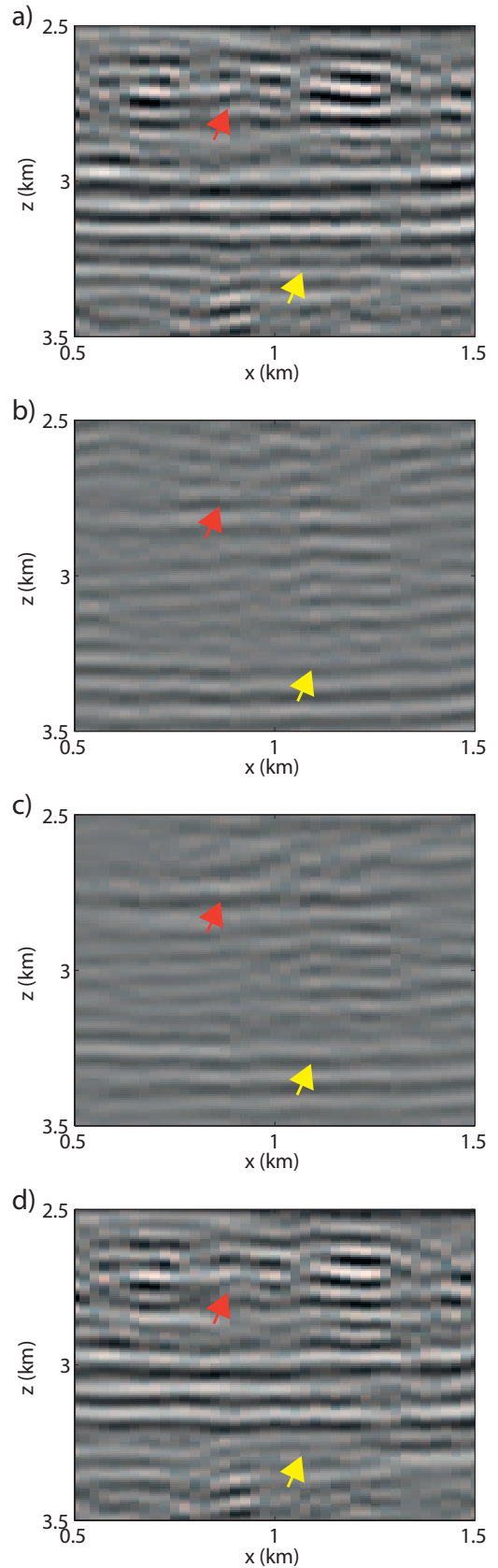


Figure 5: Zoomed sections of the blue boxes in Figures 4a, b, c and d.

## EDITED REFERENCES

Note: This reference list is a copyedited version of the reference list submitted by the author. Reference lists for the 2015 SEG Technical Program Expanded Abstracts have been copyedited so that references provided with the online metadata for each paper will achieve a high degree of linking to cited sources that appear on the Web.

## REFERENCES

- Alexandrov, D., A. Bakulin, and R. Burnstad, 2012, Virtual source redatuming of synthetic land data acquired with shallow buried receivers: 74th Conference & Exhibition, EAGE, Extended Abstracts, P252.
- Altheyab, A., X. Wang, and G. T. Schuster, 2013, Time-domain incomplete Gauss-Newton full-waveform inversion of Gulf of Mexico data: 83rd Annual International Meeting, SEG, Expanded Abstracts, 5175–5179.
- Behura, J., K. Wapenaar, and R. Snieder, 2014, Autofocus imaging: Image reconstruction based on inverse scattering theory: *Geophysics*, **79**, no. 3, A19–A26, <http://dx.doi.org/10.1190/geo2013-0398.1>.
- Berryhill, J. R., 1984, Wave-equation datuming before stack: *Geophysics*, **49**, 2064–2066, <http://dx.doi.org/10.1190/1.1441620>.
- Broggini, F., K. Wapenaar, J. van der Neut, and R. Snieder, 2014, Data-driven Green's function retrieval and application to imaging with multidimensional deconvolution: *Journal of Geophysical Research Solid Earth*, **119**, no. 1, 425–441, <http://dx.doi.org/10.1002/2013JB010544>.
- Esmersoy, C., and M. Oristaglio, 1988, Reverse-time wavefield extrapolation, imaging and inversion: *Geophysics*, **53**, 920–931, <http://dx.doi.org/10.1190/1.1442529>.
- Luo, Y., P. G. Kelamis, Q. Fu, S. Huo, G. Sindi, S. Hsu, and A. B. Weglein, 2011, Elimination of land internal multiples based on the inverse scattering series: *The Leading Edge*, **30**, 884–889, <http://dx.doi.org/10.1190/1.3626496>.
- Meles, G. A., K. Löer, M. Ravasi, A. Curtis, and C. A. da Costa Filho, 2015, Internal multiple prediction and removal using Marchenko autofocusing and seismic interferometry: *Geophysics*, **80**, no. 1, A7–A11, <http://dx.doi.org/10.1190/geo2014-0408.1>.
- Schuster, G. T., 2002, Reverse-time migration = generalized diffraction stack migration: 72nd Annual International Meeting, SEG, Expanded Abstracts, 1280–1283.
- Verschuur, D. J., 1991, Surface-related multiple elimination: An inversion approach: Ph.D. dissertation, Technical University Delft.
- Verschuur, D. J., and A. J. Berkhout, 1997, Estimation of multiple scattering by iterative inversion, Part II: Practical aspects and examples: *Geophysics*, **62**, 1596–1611, <http://dx.doi.org/10.1190/1.1444262>.
- Wapenaar, K., J. Thorbecke, J. van der Neut, F. Broggin, E. Slob, and R. Snieder, 2014, Marchenko imaging: *Geophysics*, **79**, no. 3, WA39–WA57, <http://dx.doi.org/10.1190/geo2013-0302.1>.